

# Hexahistidine-Tagged Single-Walled Carbon Nanotubes (His<sub>6</sub>-tagSWNTs): A Multifunctional Hard Template for Hierarchical Directed Self-Assembly and Nanocomposite Construction

Rachid Baati,\* Dris Ihiawakrim, Rodrigue R. Mafouana, Ovidiu Ersen, Céline Dietlin, and Guy Duportail

While a hexahistidine affinity tag can be introduced at protein termini or internal sites by standard molecular biology procedures for purification, immobilization, or labeling of proteins, here the versatility of this concept is exploited for the chemical preparation of novel hexahistidine-tagged single-walled carbon nanotubes (His<sub>6</sub>-tagSWNTs), a novel hard template useful for solubilizing, assembling, processing, and interfacing SWNTs in aqueous conditions. Water-soluble and exfoliated His<sub>6</sub>-tagSWNTs are prepared and fully characterized. This functional molecular module is able to interact via robust physisorption ( $\pi$ - $\pi$  stacking) with the sidewall of SWNTs and combines the versatility of small, water-soluble reporters (His<sub>6</sub>) for hierarchical directed self-assembly (HDSA) and construction of nanocomposites. It is demonstrated that metal coordination bonds with Ni(II) can be used for the supramolecular self assembly of His<sub>6</sub>-tagSWNTs, generating complex reticulated networks and architectures. The His<sub>6</sub>-tagSWNTs hard template nanohybrid is further utilized for directed self-assembly with silica nanoparticles. The versatility of the novel hybrids opens a new era for the rational design, smart (bio)functionalization, processing, interfacing, and self assembling of carbon nanotubes for the construction of multicomposites and more complex systems with controllable spatial organization and programmable properties for a wide range of applications in biology, nanoelectronics, and catalysis.

of nanohybrids and nanocomposites is a field of great current interest due to the potential applications of such assemblies in optoelectronics,<sup>[3]</sup> biosensing,<sup>[4]</sup> catalysis,<sup>[5]</sup> nanobiotechnology<sup>[6]</sup> and in material sciences.<sup>[7]</sup> In this context, however, the incorporation of SWCNTs into multifunctional devices still remains a difficult task due to the fact that as-produced SWCNT aggregates as large bundles and are inherently insoluble in aqueous and common organic solvents. To overcome these problems of aggregation which limit the design of elaborated CNT-based devices, efficient side-wall covalent and non-covalent strategies have been developed for the chemical functionalization of CNTs allowing the preparation of exfoliated stable suspension of SWCNTs.<sup>[8]</sup> While the covalent methods of functionalization cause undesirable disruption of the electronic and mechanical properties of SWCNTs, non-covalent approaches, based mainly on hydrophobic interactions, van der Waals interaction and  $\pi$ - $\pi$  stacking with polycyclic aromatic hydrocarbons (PAH's) such as naphthalene, phenanthrene, fluorene and pyrene,<sup>[9]</sup> are highly desirable and present numerous advantages over covalent approaches. To date a wide variety of amphiphilic molecules and biomolecules have been used for the non covalent functionalization of CNT, including, nucleic acid,<sup>[10]</sup> proteins,<sup>[9a,11]</sup> saccharides<sup>[9c,12]</sup> and peptides<sup>[13]</sup>

## 1. Introduction

Since their discovery in 1991<sup>[1]</sup> and owing to their extraordinary electronic and mechanical properties single-walled carbon nanotubes (SWCNTs) have been the subject of intensive research worldwide.<sup>[2]</sup> The use of SWCNT for the construction

Dr. R. Baati  
Functional ChemoSystem Laboratory  
University of Strasbourg  
Faculté de Pharmacie CNRS/UMR 7199  
74 route du Rhin BP 60024 67401 Illkirch, France  
E-mail: baati@bioorga.u-strasbg.fr  
D. Ihiawakrim, Dr. O. Ersen  
Université de Strasbourg  
ICPMS UMR 7504 DSI, 23 rue du Loess 67034 Strasbourg, France



Dr. R. R. Mafouana  
RBNano, 23 rue du Loess 67034 Strasbourg, France  
Dr. C. Dietlin  
Laboratoire de Photochimie et d'Ingénierie Macromoléculaires  
Université de Haute Alsace  
ENSCMu, 3 rue Alfred Werner, 68093 Mulhouse Cedex, France  
Dr. G. Duportail  
Laboratory of Biophotonics and Pharmacology  
University of Strasbourg  
Faculté de Pharmacie, CNRS/UMR 7213, 74 route du Rhin BP 60024  
67401 Illkirch, France

DOI: 10.1002/adfm.201200354

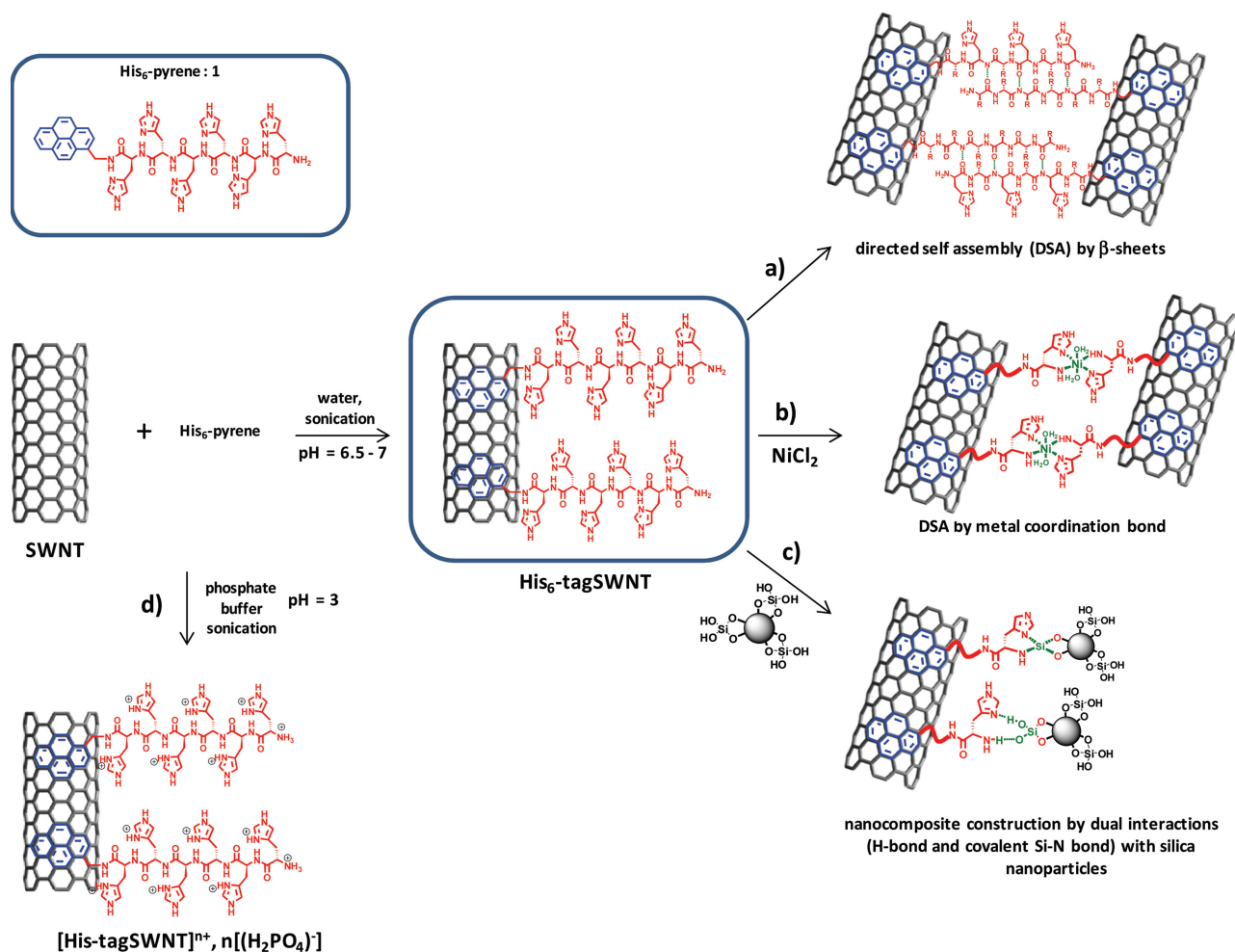


**Figure 1.** Preparation of His<sub>6</sub>-tagSWNTs, [His<sub>6</sub>-tagSWNTs]<sup>n+</sup>, n[(H<sub>2</sub>PO<sub>4</sub>)<sup>-</sup>], directed supramolecular self-assemblies, and nanocomposite construction with silica nanoparticles.

for different kind of applications. Until recently, the use of oligopeptides (MW < 2 KDa) was limited to only few examples.<sup>[14]</sup> Short peptides are extremely attractive because effective synthetic methods allow straightforward access to versatile chemical assembly of amino acids into promising engineered composites with tailored functionalities.<sup>[15]</sup> Particularly challenging would be the incorporation of polyhistidine peptides in carbon-nanotube based composites due to the versatility of this functional oligomer, inherent biocompatibility and environmental friendliness. This peptide has been widely used in chemical biology for the purification of recombinant proteins by immobilized metal affinity chromatography (IMAC) through the reversible interaction with nickel(II) nitrilotriacetic acid (NTA) binder.<sup>[16]</sup> In continuation of our interest in CNT functionalization,<sup>[9c,12e-f]</sup> we assumed that the preparation of original hydrosoluble hexahistidine-tagged CNTs (His<sub>6</sub>-tagCNTs) could be an useful molecular-scale component or template for the design and construction of novel carbon-based nanomaterials for producing innovative nanohybrids. In addition of the solubilizing properties of the hexahistidine-tag (His<sub>6</sub>-tag) in water, the biocompatible peptide could engage either hydrophobic and ionic interactions, metal coordination and covalent bonds, and hydrogen bonding for the

bottom-up elaboration of novel nanohybrids by directed self-assembly (DSA) (Figure 1).<sup>[17]</sup> Thus, by analogy with histidine-tagged proteins the oligohistidine-tag exposed at the surface of CNTs would be not only a powerful functional chemical hand offering new ways to process, interface and manipulate CNTs in pure water, but also a novel tool for the design of hard templates for nanohybrids construction.

Here we present, to the best of our knowledge, the first report on the preparation characterisation and use of hexahistidine-tagged SWCNTs (His<sub>6</sub>-tagSWNTs). We then exploited the ability of His<sub>6</sub>-tagSWNTs to self-assemble by metal coordination bonds and by directional H-bonding ( $\beta$ -sheets) to form novel organized structures and nanocomposites with silica nanoparticles, in exceptionally mild and nondestructive conditions (Figure 1), by virtue of the specific reactive sites and encoded hexahistidine information sequence.

In this study we pursued the non-covalent functionalization of CNTs with hexahistidine-based molecule. Our approach to the functionalization of CNT was to use a pyrene-hexahistidine amphiphile (HA) 1 in which the hexahistidine sequence is covalently attached to a polyaromatic pyrene tail (Figure 1, top left box). Since the surface of CNT is non polar and hydrophobic,

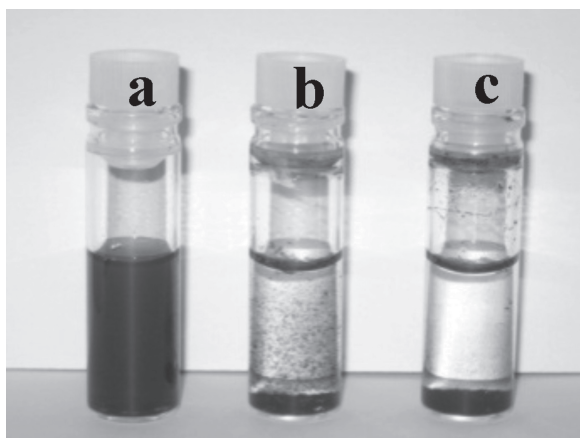


**Figure 2.** Stable aqueous dispersion (pH = 6.5–7) of His-tagSWNTs (a), non-stable dispersion of SWNT in His<sub>6</sub> aqueous solution (b), and SWCNT in deionized water (c).

HA is expected to self-assemble on the surface from aqueous solution, minimizing the interfacial energy of the CNT/water interface. This approach offers the following potential advantages: i) the hydrophobic pyrene is designed to interact with the side wall of SWNT forcing the hexahistidine sequence to be exposed towards the water; ii) the nanotube surface is not damaged chemically and the electronic and mechanical properties of CNTs are preserved; iii) the water solubility of His<sub>6</sub>-tagged SWNTs could be controlled and fine-tuned either by H-bonding, coordination with metals, or by adjusting the pH; and iv) the multivalency of the tag would allow the reversible anchoring and interfacing with any kind of synthetic molecule, biomolecule, drug or nanomaterial. Our approach using multifunctional molecular module hexahistidine peptide is expected to have a wide scope of application in the construction of miniaturized novel nanoconstructs and CNT-based bionanodevices.

## 2. Results and Discussion

SWNTs (0.5 mg) were first reacted with N-termini NH<sub>2</sub>-His<sub>6</sub>-pyrene amphiphile **1** (C = 1 mg/mL) dissolved in 1 mL of deionized water at pH = 6.5–7 (Figure 1). Upon sonication for 1 h using simply a water bath at room temperature (see Supporting Information) a stable black aqueous dispersion of SWNTs is obtained as can be seen by the naked eye (Figure 2, vial a). We dubbed SWCNTs coated with (poly)-hexahistidine tags: His<sub>6</sub>-tagSWNTs. Control experiment using hexahistidine peptide (His<sub>6</sub>, C = 1 mg/mL) in deionized water lacking the hydrophobic pyrene tail moiety had no solubilizing effect on SWNTs (Figure 2, vial b).

These results clearly demonstrate the high dispersion ability of NH<sub>2</sub>-His<sub>6</sub>-pyrene amphiphile **1**, and the fact that the aromatic imidazole residues of the hexahistidine

peptide **1** does not interact strongly via  $\pi$ - $\pi$  stacking with the hydrophobic side wall of the nanotube, in sharp contrast with precedent reports.<sup>[13a]</sup> Indeed,  $\pi$ - $\pi$  interactions between the aromatic amino acids (histidine, tryptophane and tyrosine) of polypeptides and the extended  $\pi$ -electron system of SWCNT is considered to be the main driving force for specific phage display polypeptide adsorption onto SWCNT.<sup>[13a]</sup> In our case, we found that the His<sub>6</sub> peptide alone does not afford stable dispersion of SWCNT (Figure 2, vial b), meaning that the efficiency of the functionalization and dispersion in water is exclusively ascribed to the amphiphilic character of NH<sub>2</sub>-His<sub>6</sub>-pyrene **1** and the high propensity of pyrene to stick on the SWNT surface (binding energy of pyrene to the surface of SWCNT  $\approx$  9.7 kcal mol<sup>-1</sup>),<sup>[18]</sup> the hydrophilic His<sub>6</sub> peptide assuring the aqueous solubility and stability in water. His<sub>6</sub>-tagSWNTs and small His<sub>6</sub>-tagged bundles obtained and dissolved in this fashion were stable toward aggregation over the course of weeks. Notably, as a result of directional hydrogen bonding between the His<sub>6</sub> tags at the surface of SWNTs, leading most likely to  $\beta$ -sheets by lateral association,<sup>[19]</sup> kinetically slow directed self-assembling of the nanotubes occurs, resulting to partial supramolecular aggregation, while maintaining a quite stable aqueous suspensions (Figure 1, reaction a). These molecular-recognition driven assemblies are reminiscent with what has been described very recently for nucleobase hybrid nanotubes.<sup>[20]</sup> High resolution transmission electron microscopy (HRTEM) provides insight into the morphology of the newly prepared His<sub>6</sub>-tagSWNTs (Figure 3a,b) as well as His<sub>6</sub> tagged supramolecular SWNT aggregates (Figure 3c).

Inspection of the HRTEM images of His<sub>6</sub>-tagSWNTs sample reveals a certain degree of debundling induced by NH<sub>2</sub>-His<sub>6</sub>-pyrene amphiphile **1** (Figure 3a,b). The nanotubes appeared somehow thickened with a blur on their surface, most likely by the pyrene hexahistidine tag (Figure 3b).

His<sub>6</sub>-tagSWNTs samples were characterized by using laser Raman spectroscopy to obtain the degree of defects of the nanotube surface eventually caused during the preparation process induced by sonication. Typical Raman spectra excited

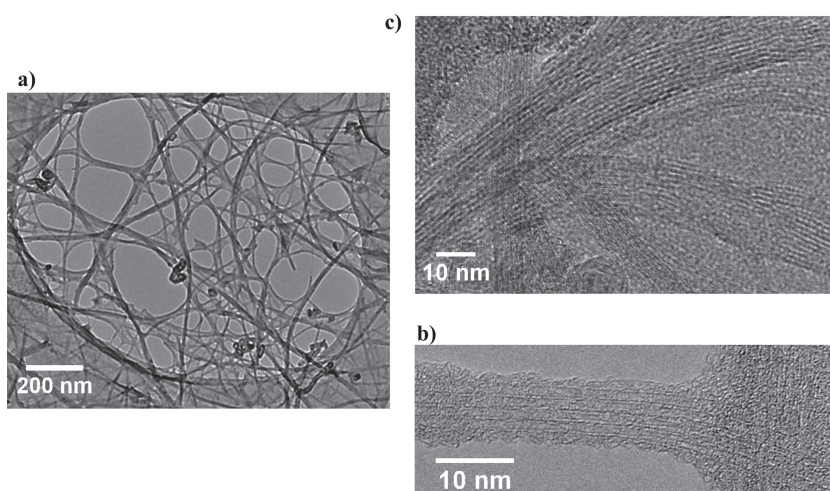


**Figure 3.** HRTEM image of His<sub>6</sub>-tagSWNTs (a,b) and His<sub>6</sub>-tagged supramolecular SWNTs aggregates (c).

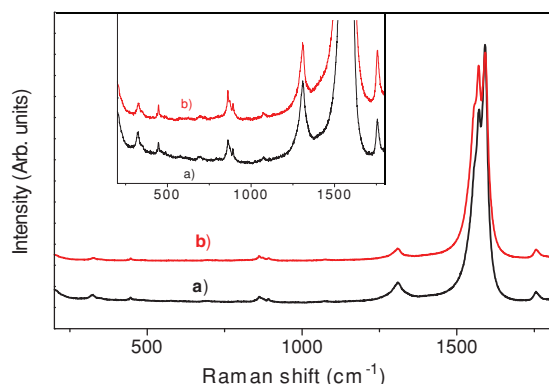


**Figure 4.** Raman spectra with excitation at  $\lambda = 785$  nm of non functionalized SWNTs (a) and His<sub>6</sub>-tagSWNTs (b)

at 785 nm and normalized at the G band intensity of non functionalized SWNT and His<sub>6</sub>-tagSWNT are shown in **Figure 4**. As could be expected, side-wall of non-covalently functionalized His<sub>6</sub>-tagSWNT (b) was not altered since the relative intensity of the disorder D band (1280–1320 nm) does not increase as compared to the one obtained for non functionalized SWNT (a).

This also implies that the electronic structure of the His<sub>6</sub>-tagSWNTs remains intact after being non-covalently functionalized with NH<sub>2</sub>-His<sub>6</sub>-pyrene amphiphile **1**. His<sub>6</sub>-tagSWNTs were also characterized by their absorption spectra and their excitation and emission fluorescence spectra. Using pyrene-hexahistidine conjugate **1** as a solubilizer, the aqueous solution of SWNTs changed from colorless to black, implying the solubilisation of SWNTs. The UV-Vis absorption spectra of **1** in water (**Figure 5**) displays the characteristic features of pyrene absorbance, with the well known and repetitive vibronic structure of the two main electronic transitions in the absorption spectrum, corresponding to the excitation to the second and third singlet excited states. Upon  $\pi$ - $\pi$  stacking of the pyrene moiety of **1** to the graphene surface of SWNTs, the sharp and distinct vibronic structures of the absorption bands are no longer well

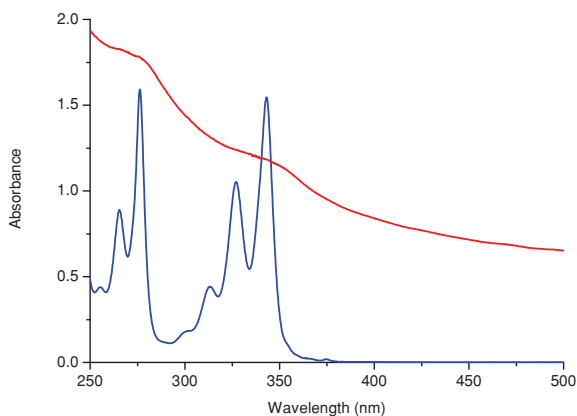


**Figure 5.** Absorption spectra of NH<sub>2</sub>-His<sub>6</sub>-pyrene **1** (blue) and for a stable aqueous dispersion of His<sub>6</sub>-tagSWNTs (red). Concentration of **1** = 95  $\mu$ M; concentration of SWNT  $\approx$  50  $\mu$ g/mL.

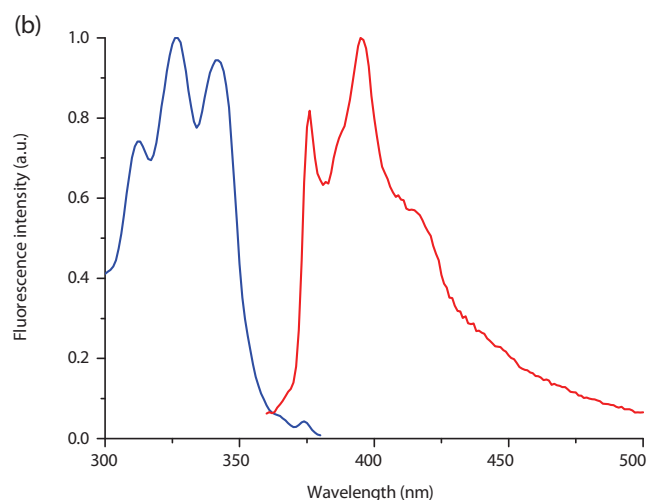
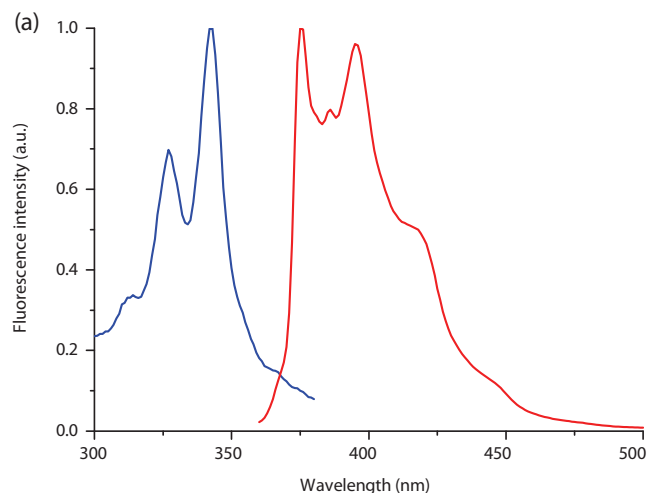


**Figure 6.** Normalized fluorescence excitation (blue) and emission (red) spectra of **1** (a) and a stable aqueous dispersion of His<sub>6</sub>-tagSWNTs (b). Excitation wavelength: 335 nm; emission wavelength: 400 nm; band-width: 2 nm.

resolved, as they appear only as shoulders, with a considerably lower absorbance, from the absorption background due to the proper absorbance and light scattering of dissolved SWNTs. This hypochromicity of the absorption bands remains difficult to quantify due to probable screening effects.

The fluorescence spectra, both in excitation and emission, are also giving a direct evidence for the interaction of the pyrene moiety to the sidewall of the SWNTs (**Figure 6**). The emission spectrum of His<sub>6</sub>-pyrene in water is roughly similar with the one of pyrene in identical condition,<sup>[21]</sup> with just a decrease of the relative intensity of the emission peak at 390 nm. Comparatively, the stacking of hexahistidine pyrene **1** on SWNTs induces a strong modification of the vibronic structure of the emission spectrum. This spectrum is practically identical to the one previously obtained for a SWNT-based pH sensor containing a pyrene moiety.<sup>[22]</sup> Such a profile of emission spectrum probably reflects the unsymmetrical environment of the pyrene ring, apolar on the graphene side and polar to the bulk water side.



Together with this modification of the emission profile, a substantial quenching of fluorescence, of about two orders of magnitude (not shown), is resulting from the interaction of **1** and SWNTs. Such a fluorescence quenching was previously observed with other SWNT-pyrene functionalized composites and was explained through some energy transfer mechanisms or coupling between energy levels from the photoexcited electrons of the pyrene moieties to empty electronic states of the SWNTs.<sup>[22–24]</sup> Also, the vibronic structure of the corresponding excitation spectrum for His<sub>6</sub>-tagSWNTs appears quite smoothened as compared to the excitation spectrum of amphiphile **1** in water with closer amplitudes of the different pyrene vibrational modes, which in some way can rely to the loss of the vibronic structure observed in the absorption spectrum.

FTIR of His<sub>6</sub>-tagSWNTs (see Supporting Information) shows the presence of the amide group ( $\nu_{\text{CO}} = 1669 \text{ cm}^{-1}$ ) and two bands characteristic of the free amino group ( $\nu_{\text{N-H}} = 3182 \text{ cm}^{-1}$  and  $1455 \text{ cm}^{-1}$ ). The degree of functionalization was further probed by thermogravimetric analysis. TGA of His-tagged SWNTs show a weight loss of 28% at 200 °C compared to unfunctionalized SWNTs (see Supporting Information). At this temperature regime the organic His<sub>6</sub>-tag is almost fully removed, while the SWNTs remains intact (data not shown). Notably, positive Kaiser Test performed on a stable suspension of aqueous His<sub>6</sub>-tagSWNTs demonstrated qualitatively the presence of  $-\text{NH}_2$  groups arising from the N-termini His<sub>6</sub>-tag at the surface of SWNTs.<sup>[25]</sup> This amino- chemical function could offer many possibilities for further covalent and ionic functionalisation by surface chemistry. Finally we also demonstrated that the functionalization of SWNTs is effective upon sonication in acidic conditions (pH = 3, phosphate buffer) with polycationic amphiphile **1** (Figure 1d), allowing the synthesis of  $[\text{His}_6\text{-tagSWNT}]^{\text{p}+}$ . This novel polycationic nanohybrid opens new perspectives and avenues for self-assemblies with polyanionic molecules, including DNA/RNA or siRNA for transfection applications, heparin derivatives and anionic polymers by virtue of layer-by-layer (LbL) interactions.<sup>[26]</sup>

To demonstrate further the utility of His<sub>6</sub>-tagged SWNTs we first used the peptide-code (encoded information) of the His<sub>6</sub>-tag at the surface of the nanotube to direct self assembling of SWNT triggered by metal coordination bonds. Recently,

by means of isothermal calorimetry (ITC) measurements our research group demonstrated that  $\text{Ni}^{2+}$  exhibited a strong affinity for hexahistidine oligopeptide by generating His<sub>6</sub>-Ni<sup>(II)</sup>-His<sub>6</sub> symmetrical ternary complexes.<sup>[16f]</sup> In light of our findings we envisioned to investigate this unexplored property of polyhistidine to promote supramolecular self-assembly of carbon nanotubes, *via* metal coordination bonds, upon reaction of His<sub>6</sub>-tagSWNTs with Ni(II) chloride in aqueous conditions. Experimentally, the treatment of a stable aqueous dispersion of His<sub>6</sub>-tagSWNTs with an aqueous solution of  $\text{NiCl}_2$  led to the formation of microscopically ordered nanostructures which resulted in a spontaneous aggregation of large insoluble aggregates (Figure 7 and Supporting Information).

This result suggests that the metal ion is coordinated most likely in sandwich fashion at the N-termini of two histidine tags, as shown schematically in Figure 1b, leading to the tight self-assembly of SWNTs in larger structured networks (Figure 7a,b). While the exact binding mechanism remains elusive, it is likely that Ni(II) is coordinated through a two-site coordination manner by each tag acting as a functional bridge (Figure 1b). The use of metal-ligand interaction in the construction of coordinated peptide-based SWNTs represents a challenging strategy for the elaboration of miniaturized metal sensors. Encouraged by this result, we next investigated the feasibility of utilizing His<sub>6</sub>-tagSWNTs in the construction of composites nanomaterials through H-bonding and/or covalent bond interactions with the objective to control the precise molecular architecture at a nanometer scale. To demonstrate the proof of principle, we chose silica nanoparticles that offer the possibility for H-bonding and covalent bond opportunities due to the silanol functionalities on their outer surface for the generation of nanocomposites. In a typical experiment, a stable aqueous suspension of His<sub>6</sub>-TagSWNTs is simply mixed at room temperature with a homogeneous aqueous dispersion of silica nanoparticles (see Supporting Information). While we could eventually anticipate a spontaneous aggregation and precipitation of complex nanostructures, as it was the case for the reaction with Ni(II), the homogenous His<sub>6</sub>-tagSWNTs dispersion remained stable upon addition and self-assembly with the silica nanoparticles. This result could be easily observed and followed by the naked eye (see Supporting Information), and the stability of the dispersion is ascribed to the high surface area of the nanocomposites and therefore the high degree

of its solvation by the surrounding solvent water molecules. The excellent stability of the dispersion presumably relies on a subtle balance of “internanoparticles” H-bonding and/or covalent interactions versus intermolecular H-bonding ones between the entire nanocomposite (His<sub>6</sub>-tagSWNTs/SiO<sub>2</sub>) with solvent water molecules. Further theoretical studies devoted to the understanding of the stability and solubility of the nanocomposites in water dispersion are under investigation.

Cryo-HRTEM analysis of the sample revealed the smart interfacing of SWNTs with silica nanoparticles thanks to the encoded His-tag information leading through hierarchical self assembly to novel His<sub>6</sub>-tagSWNTs/SiO<sub>2</sub>

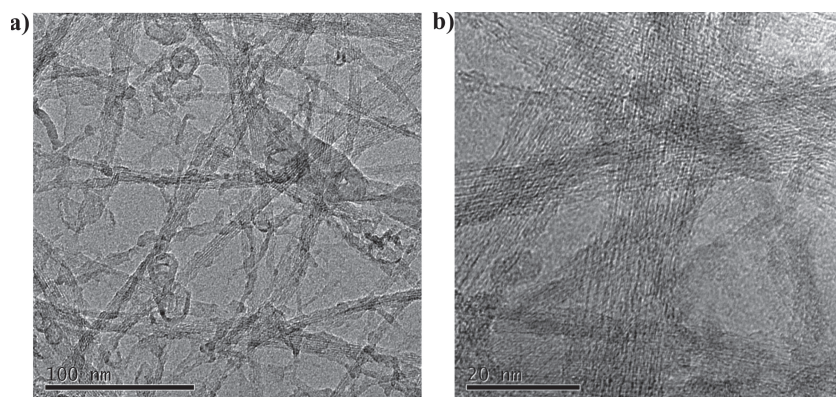


**Figure 7.** Two typical high resolution-TEM images of self-assembled structures of His<sub>6</sub>-tagSWNTs/(Ni<sup>2+</sup>)<sub>n</sub>/His<sub>6</sub>-tagSWNTs.

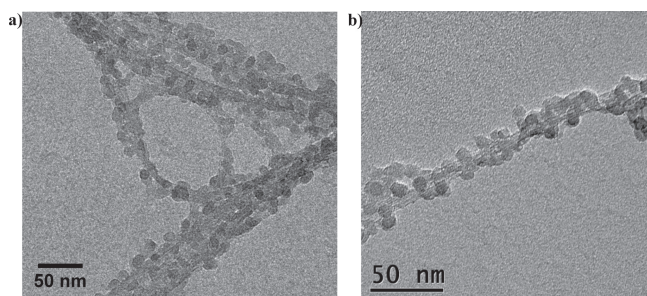


**Figure 8.** Representative TEM pictures of His-tagSWNTs/SiO<sub>2</sub>, taken at low temperature on different magnifications.

nanocomposites (Figure 1d and Figure 8). Control experiments carried out with unfunctionalized hydrophobic SWNTs and the same aqueous solution of hydrophilic silica nanoparticles failed to provide any stable analyzable nanoconstruct, demonstrating the unique physico-chemical features of the His<sub>6</sub>-pyrene amphiphilic conjugate in our stepwise bottom-up approach for the generation of novel water soluble nanocomposites.

To characterize His<sub>6</sub>-tagSWNTs/SiO<sub>2</sub> nanocomposites from chemical point of view, electron energy loss spectroscopy (EELS, see Supporting Information) measurements have been performed on typical areas of the sample, such as that represented on Figure 8b. A representative EELS spectrum is shown in the Supporting Information and illustrates the presence of carbon, silicon and oxygen (from SiO<sub>2</sub> nanoparticles) and nitrogen characteristic for the occurrence of hexahistidine-based molecule. This novel nanohybrids could be further functionalized and find novel applications as nanoprobe for biomedical and theranostic imaging or in the elaboration of more complex nanoconstructs for material sciences and catalysis.

### 3. Conclusion

In summary, we have successfully extended the concept of “His<sub>6</sub>-tagged proteins” used in chemical biology (for handling and purification of proteins) for the synthetic generation of novel processable “His<sub>6</sub>-tagSWNTs” nanoconstruct. The unique characteristics of our process relying on the use of biocompatible pyrene-hexahistidine amphiphiles is the achievement of stable aqueous dispersion of His<sub>6</sub>-tagSWNTs without using drastic conditions or hazardous reagents. By means of the chemical non-covalent and non-destructive functionalization of SWNTs we demonstrated that His<sub>6</sub>-tagSWNTs represent a unique hard template endowed with remarkable and versatile chemical properties induced by the peptide-code, such as hierarchical directed self-assembly driven either by H-bonding ( $\beta$ -sheets), coordination bonds with Ni(II) or covalent interactions. These intrinsic properties efficiently allowed the preparation of SWNT/His<sub>6</sub>/Ni(II)<sub>n</sub>/His<sub>6</sub>/SWNT networks and water soluble His<sub>6</sub>-tagSWNTs/SiO<sub>2</sub> nanocomposites by spontaneous directed self-assembly. The set of results described in this article is highly promising and demonstrated that oligo-histidine tags could potentially be used for interfacing, immobilization and processing hydrophobic carbon nanotubes with a large variety of synthetic nanoparticles, that may find a wide

range of applications in nanomedicine, catalysis, material science, and nanoelectronic. The biological evaluation (toxicity, biodistribution, etc.) of His<sub>6</sub>-tagSWNTs and related nanocomposites, are currently investigated in our laboratories and will be reported shortly.

### Supporting Information

Supporting Information is available from the Wiley Online Library or from the author. Experimental procedures for the functionalisation of SWNTs with NH<sub>2</sub>-His<sub>6</sub>-pyrene 1, preparation of aggregates with Ni(II) Cl<sub>2</sub>, and self-assembly protocols for the construction of nanocomposites with SiO<sub>2</sub> nanoparticles are described. MS and HPLC analysis for NH<sub>2</sub>-His<sub>6</sub>-pyrene 1 are provided. Raman, IR, and TGA analysis for His-tagSWNTs are also reported. EELS experiments and a HRTEM image of His-tagSWNTs/SiO<sub>2</sub> nanocomposite are also given.

### Acknowledgements

R.B. is grateful to the CNRS and to the University of Strasbourg for a grant on the functionalization of CNT with biomolecules (PICS n°4456). Dr. Ileana Florea and Didier Burger from IPCMS (UdS) are gratefully acknowledged for fruitful discussions, EELS measurements, and for the ATG experiments.

Received: February 6, 2012  
Published online: June 4, 2012

- [1] S. Iijima, T. Ichhashi, *Nature* **1993**, 363, 603.
- [2] N. Karousis, N. Tagmatarchis, *Chem. Rev.* **2010**, 110, 5366.
- [3] B. S. Shim, Z. Tang, M. P. Morabito, A. Agarwal, H. Hong, N. A. Kotov, *Chem. Mater.* **2007**, 19, 5467.
- [4] a) N. F. Reuel, J.-H. Ahn, J.-H. Kim, J. Zhang, A. A. Boghossian, L. K. Mahal, M. S. Strano, *J. Am. Chem. Soc.* **2011**, 133, 17923; b) X. Xu, S. Jiang, Z. Hu, S. Liu, *ACS Nano* **2010**, 4, 4292.
- [5] a) J. John, E. Gravel, A. Hagège, H. Li, T. Gacoin, E. Doris, *Angew. Chem. Int. Ed.* **2011**, 50, 7533; b) P. Singh, G. Lamanna, C. Ménard-Moyon, F. Maria Toma, E. Magnano, F. Bondino, M. Prato, S. Verma, A. Bianco, *Angew. Chem. Int. Ed.* **2011**, 50, 9893.
- [6] a) M. Bottini, N. Rosato, N. Bottini, *Biomacromolecules.* **2011**, 12, 3381; b) K. Kostarelas, A. Bianco, M. Prato, *Nat. Nanotechnol.* **2009**, 4, 627.
- [7] a) K. Matsumoto, T. Fujigaya, K. Sasaki, N. Nakashima, *J. Mater. Chem.* **2011**, 21, 1187; b) Y. Lin, K. A. Watson, M. J. Fallbach, S. Ghose, J. G. Smith Jr., D. M. Delozier, W. Cao, R. E. Crooks, J. W. Connell, *ACS Nano* **2009**, 3, 871.
- [8] D. Tasis, N. Tagmatarchis, A. Bianco, M. Prato, *Chem. Rev.* **2006**, 106, 1105.
- [9] a) R. J. Chen, Y. Zhang, D. Wang, H. Dai, *J. Am. Chem. Soc.* **2001**, 123, 3838; b) J. Zhang, J.-K. Lee, Y. Wu, R. W. Murray, *Nano Lett.* **2003**, 3, 403; c) M. Assali, M. P. Leal, I. Fernandez, P. Romero-Gomez, R. Baati, N. Khier, *Nano Res.* **2010**, 3, 764.
- [10] a) M. Zheng, A. Jagota, E. D. Semke, B. A. Diner, R. S. Mclean, S. R. Lustig, R. E. Richardson, N. G. Tassi, *Nat. Mater.* **2003**, 2, 338; b) M. Zheng, A. Jagota, M. S. Strano, A. P. Santos, P. Barone, S. G. Chou, B. A. Diner, M. S. Dresselhaus, R. S. McLean, G. B. Onoa, G. G. Samsonidze, E. D. Semke, M. Usrey, D. J. Walls, *Science* **2003**, 302, 1545.

- [11] a) G. R. Dieckmann, A. B. Dalton, P. A. Johnson, J. Razal, J. Chen, G. M. Giordano, E. Munoz, I. H. Musselman, R. H. Baughman, R. K. Draper, *J. Am. Chem. Soc.* **2003**, 125, 1770; b) S. S. Karajanagi, H. C. Yang, P. Asuri, E. Sellitto, J. S. Dordick, R. S. Kane, *Langmuir* **2006**, 22, 1392.
- [12] a) X. Chen, G. S. Lee, A. Zettl, C. R. Bertozzi, *Angew. Chem. Int. Ed.* **2004**, 43, 6111; b) M. Numata, M. Asai, K. Kaneko, A. H. Bae, T. Hasegawa, K. Sakurai, S. Shinkai, *J. Am. Chem. Soc.* **2005**, 127, 5875; c) X. Chen, U. C. Tam, J. L. Czapinski, G. S. Lee, D. Rabuka, A. Zettl, C. R. Bertozzi, *J. Am. Chem. Soc.* **2006**, 128, 6292; d) P. Wu, X. Chen, N. Hu, U. C. Tam, O. Blixt, A. Zettl, C. R. Bertozzi, *Angew. Chem. Int. Ed.* **2008**, 47, 5022; e) N. Khair, M. Pernia Leal, R. Baati, C. Ruhlmann, C. Mioskowski, P. Schultz, I. Fernandez, *Chem. Commun.* **2009**, 4121; f) M. Assali, M. Pernia Leal, I. Fernández, R. Baati, C. Mioskowski, N. Khair, *Soft Matter* **2009**, 5, 948.
- [13] a) S. Wang, E. S. Humphrays, S.-Y. Chung, D. F. Delduco, S. R. Lustig, H. Wang, K. N. Parker, N. W. Rizzo, S. Subramoney, Y.-M. Chiang, A. Jagota, *Nat. Mater.* **2003**, 2, 196; b) V. Zorbas, A. Ortiz-Acevedo, A. B. Dalton, M. M. Yoshida, G. R. Dieckmann, R. K. Draper, R. H. Baughman, M. Jose-Yacamán, I. H. Musselman, *J. Am. Chem. Soc.* **2004**, 126, 7222; d) G. R. Dieckmann, A. B. Dalton, P. A. Johnson, J. Razal, J. Chen, G. M. Giordano, E. Munoz, I. H. Musselman, R. H. Baughman, R. K. Draper, *J. Am. Chem. Soc.* **2003**, 125, 1770; e) A. Ortiz-Acevedo, H. Xie, V. Zorbas, W. M. Sampson, A. B. Dalton, R. Baughman, R. K. Draper, I. H. Musselman, G. R. Dieckmann, *J. Am. Chem. Soc.* **2005**, 127, 9512; f) C. G. Salzman, M. A. H. Ward, R. M. J. Jacobs, G. Tobias, M. L. H. Green, *J. Phys. Chem. C* **2007**, 111, 18520; g) G. K.-C. Lee, M. A. H. Ward, B. T. T. Chu, M. L. H. Green, *J. Mater. Chem.* **2008**, 18, 1977; h) H. Xie, A. Ortiz-Acevedo, V. Zorbas, R. H. Baughman, R. K. Draper, I. H. Musselman, A. B. Dalton, G. R. Dieckmann, *J. Mater. Chem.* **2005**, 15, 1734; j) L. S. Witus, J.-D. R. Rocha, V. M. Yuwono, S. E. Paramonov, R. B. Weisman, J. D. Hartgerink, *J. Mater. Chem.* **2007**, 17, 1909.
- [14] M. S. Arnold, M. O. Guler, M. C. Hersam, S. I. Stupp, *Langmuir* **2005**, 21, 4705.
- [15] a) M. R. Ghadiri, J. R. Granja, R. A. Milligan, D. E. McRee, N. Khazanovich, *Nature* **1993**, 366, 324; b) X. Yan, P. Zhua, J. Li, *Chem. Soc. Rev.* **2010**, 39, 1877.
- [16] a) E. Hochuli, H. Dobeli, A. Schacher, *J. Chromatogr.* **1987**, 411, 177; b) E. K. Ueda, P. W. Gout, L. Morganti, *J. Chromatogr. A* **2003**, 988, 1; c) C. Hart, B. Schulenberg, Z. Diwu, W. Y. Leung, W. F. Patton, *Electrophoresis* **2003**, 24, 599; d) J. Kim, H.-Y. Park, J. Kim, J. Ryu, Y. Kwon, R. Do, R. Grailhe, C. Song, *Chem. Commun.* **2008**, 1910; e) W. Shen, H. Zong, D. Neff, M. Norton, *J. Am. Chem. Soc.* **2009**, 131, 6660; f) M. Brellier, B. Barlaam, C. Mioskowski, R. Baati, *Chem. Eur. J.* **2009**, 46, 12689.
- [17] S. Li, P. He, J. Dong, Z. Guo, L. Dai, *J. Am. Chem. Soc.* **2005**, 127, 14.
- [18] S. Cavalli, F. Albericio, A. Kros, *Chem. Soc. Rev.* **2010**, 39, 241.
- [19] a) M. Quintana, M. Prato, *Chem. Commun.* **2009**, 6005; b) P. Singh, F. M. Toma, J. Kumar, V. Venjatesh, J. Raya, M. Prato, B. Febre, S. Verma, A. Bianco, *Chem. Eur. J.* **2011**, 17, 6772; c) P. Singh, J. Kumar, F. M. Toma, J. Raya, M. Prato, B. Febre, S. Verma, A. Bianco, *J. Am. Chem. Soc.* **2009**, 131, 13555; d) M. Quintana, H. Traboulsi, A. Llanes-Pallas, R. Marega, D. Bonifazi, M. Prato, *ACS Nano* **2012**, 6, 23.
- [20] P. G. Holder, M. B. Francis, *Angew. Chem. Int. Ed.* **2007**, 46, 4370.
- [21] P. Lianos, S. Gheorghiou, *Photochem. Photobiol.* **1979**, 30, 355.
- [22] E. S. Cho, S. W. Hong, W. H. Jo, *Macromol. Rapid Commun.* **2008**, 29, 1798.
- [23] L. Qu, R. B. Martin, W. Huang, K. Fu, D. Zweifel, Y. Lin, Y.-P. Sun, C. E. Bunker, B. A. Harruff, J. R. Gord, L. F. Allard, *J. Chem. Phys.* **2002**, 117, 8089.
- [24] C. F. Chiu, N. Dementev, E. Borguet, *J. Phys. Chem. C* **2011**, 115, 9579.
- [25] E. Kaiser, R. L. Colescot, C. D. Bossing, P. I. Cook, *Anal. Biochem.* **1970**, 34, 595.
- [26] G. Decher, *Science* **1997**, 277, 1232.